Photosynthesis Research
https://doi.org/10.1007/s11120-022-00915-w

ORIGINAL ARTICLE

Light-harvesting complex gene regulation by a MYB-family transcription factor in the marine diatom, *Phaeodactylum tricornutum*

Ananya Agarwal[1,2] · **Rong Di**[3] · **Paul G. Falkowski**[1,4]

Received: 18 October 2021 / Accepted: 16 March 2022

Abstract

Unicellular photoautotrophs adapt to variations in light intensity by changing the abundance of light harvest pigment-protein complexes (LHCs) on time scales of hours to days. This process requires a feedback signal between the plastid (where light intensity is sensed) to the nucleus (where the genes for LHCs are encoded). The signals must include heretofore unidentified transcription factors that modify the expression level of the LHCs. Analysis of the nuclear genome of the model diatom *Phaeodactylum tricornutum* revealed that all the *lhc* genes have potential binding sites for transcription factors belonging to the MYB-family proteins. Functional studies involving antisense RNA interference of a hypothetical protein with a MYB DNA-binding domain were performed. The resultant strains with altered photosynthetic and physiological characteristics lost their ability to acclimate to changes in irradiance; i.e., cellular chlorophyll content became independent of growth irradiance. Our results strongly suggest that the inter-organellar signaling cascade was disrupted, and the cell could no longer communicate the environmental signal from the plastid to the nucleus. Here, we identify, for the first time, an LHC Regulating Myb (LRM) transcription factor, which we propose is involved in *lhc* gene regulation and photoacclimation mechanisms in response to changes in light intensity.

Keywords Diatom · Phaeodactylum · Light intensity · Photoacclimation · MYB · Transcription factor · Light harvesting complex LHC · Signaling

Introduction

The most important environmental cue for unicellular photosynthetic organisms is light. In response to light stress, photoautotrophs have evolved an extensive array of mechanisms and cellular adaptations to maintain optimal cellular efficiency (Falkowski and LaRoche 1991; Long, et al. 1994). Physiologically, these consist of light sensing mechanisms that trigger signal transduction processes from the environment to the plastid to the nucleus (Hegemann et al., 2001; Nott et al. 2006). These so-called retrograde signaling responses, involve feedbacks that modify transcription and translation profiles of nuclear, plastid and, in some cases, mitochondrial genomes (e.g., Escoubas et al. 1995). The molecules involved in the signaling are very poorly understood. While a few of the signal transduction mechanisms have been elucidated in model organisms of higher plants and green algae (Meyerowitz 2001; Zallen 1993; Rochaix 1995; Glatz et al. 1999; Grossman 2000; Harris 2001), they remain obscure in secondary symbionts, such as diatoms, which have a different evolutionary history (Falkowski et al. 2004).

Some of the observed, reversible, phenotypic changes in response to changes in irradiance, result from the differential expression of proteins involved in various biosynthetic processes (Pfannschmidt 2003). Changing the concentration of macromolecules/proteins such as light harvesting pigment-protein complexes, components of the electron transport chain, photoreceptors, accessory carotenoids, help the cell to compensate for any damage

✉ Paul G. Falkowski
falko@marine.rutgers.edu

1 Environmental Biophysics and Molecular Ecology Program, Department of Marine and Coastal Sciences, Rutgers University, New Brunswick, NJ, USA

2 Department of Biochemistry and Microbiology, Rutgers University, New Brunswick, NJ, USA

3 Department of Plant Biology, Rutgers University, New Brunswick, NJ, USA

4 Department of Earth and Planetary Sciences, Rutgers University, Piscataway, NJ, USA

Published online: 07 April 2022

or insufficiency induced by spectral fluctuations (Durnford and Falkowski 1997; Falkowski and LaRoche 1991; Pfannschmidt et al. 2009; Sukenik et al. 1987).

Here we focus on an acclimation mechanism that, unlike the short-term transient compensatory mechanisms such as state transitions or non-photochemical quenching (e.g., Long et al. 1994; Buck et al. 2019), involves changing the expression of specific genes (Escoubas et al. 1995). In diatoms, the light harvesting pigment proteins are encoded in the nuclear genome (Büchel 2019). Under low light, the expression of these genes is upregulated, while under high light they are down regulated (Levitan et al. 2015; Dinamarca et al. 2017). How light regulates the expression of these genes is not understood.

The physiology and metabolism of all organisms are regulated by the action of Transcription Factors (TF's) on various genes. This control at the level of transcription, allows the organism to adapt to variable environments. Complex organisms like eukaryotes, having multiple organellar genomes, possess a large number of TF's that can be classified into different families based on their DNA-binding domains. In Rayko et al. 2010, several transcription factors in the model marine diatom, *Phaeodactylum tricornutum* were identified. However, transcriptional control mechanisms, particularly associated with environmental stress acclimation currently remain poorly understood. Although we have identified 575 putative transcription factors in a strain of *P. tricornutom* from various databases (NCBI GEO Accession # GSE133301), the function of the vast majority of these genes of have yet to be characterized (Matthijs et al. 2017).

In higher plants, one of the largest transcription factor families are the MYB-like proteins (Lindemose et al. 2013). These signaling proteins, especially the R2R3-type in terrestrial plants, are involved in a variety of processes. MYBs have been identified in low temperature acclimation (Soitamo et al. 2008), stomatal aperture control (Liang et al. 2005), as well as drought response signaling by changing chlorophyll biosynthesis enzyme expression (Liu et al. 2018). With respect to photosynthesis, a MYB associated with the circadian clock was found to regulate phytochrome induction of light harvesting chlorophyll synthesis in *A. thaliana* (Wang and Tobin 1998). Further, MYBs have been identified in phytochrome A-initiated signal transduction responses to far-red light (Ballesteros et al. 2001), regulate chlorophyll a/b-binding (CAB) gene expression in response to a variety of environmental triggers (Churin et al. 2003), photosynthetic gene expression regulation (Zhou and Li 2016) as well as controlling flavonoid biosynthesis (Zoratti et al. 2014; Albert et al. 2009).

P. tricornutum has 34 characterized and 7 uncharacterized *lhc* genes, that can be distinguished into the F, R, and X-family types (DiatomCyc database—www.diatomcyc.org).

Here we investigate light intensity-stimulated gene expression regulation of light harvesting complex genes *P. tricornutum*, and the potential role of a MYB-type transcription factor in the retrograde signaling cascade.

Materials and methods

Growth conditions and maintenance

The pennate marine diatom, *Phaeodactylum tricornutum* (accession Pt1 8.6; CCMP 632 in the Provasoli-Guillard National Center for Marine Algae and Microbiota) (De Martino et al. 2007) was maintained axenically in sterile artificial seawater (Goldman and McCarthy 1978; McLachlan 1964) enriched with F/2 nutrients (Guillard and Ryther 1962) in the absence of Si. A set of three, optically thin, biologically independent, cultures was maintained under exponential growth conditions starting at 1×10^5 cells/mL in UltraCruz flasks at 18 °C. These were grown in continuous white light from light emitting diodes (LEDs), and acclimated to specific intensities of constant light of 20 and 750–800 µmol photons m^{-2} s^{-1}. Exponentially growing cultures were kept optically thin for at least three days before and during sampling for each experiment. All transformants were maintained under the same conditions as the WT and supplemented with 100 µg/mL Zeocin™ Selection Reagent (R25005; ThermoFisher Scientific, MA) to maintain constant selection pressure.

RNAi plasmid design and transformation in WT

A linearized backbone was made by digesting a pBluescript based plasmid with XbaI & EcoRI (Supplemental Plasmid Map S1). Sequences coding for interfering RNA (iRNA) fragments were designed to target the functional domains of Phatr3_EG02570 based on NCBI BLAST annotations of conserved functional domains (blast.ncbi.nlm.nih.gov/ Blast; www.ncbi.nlm.nih.gov/Structure). The 343 bp sequence fragment was amplified from the wild type *P. tricornutum* genome (Supplemental Table S4) which regenerated the *Xba*I and *Eco*RI sites.

To achieve interference of translation of the target gene, this sequence fragment was inserted into the plasmid in the reverse complement orientation to make a pKS-H4B-ShBle-Phatr3_EG02570(antisense)-FA vector using a Gibson Assembly® Cloning Kit (E5510S New England Biolabs, MA; Gibson et al. 2009, 2010). This vector was propagated using heat shock transformation of One Shot TOP10 Chemically Competent Escherichia coli (C404010; ThermoFisher Scientific, MA) and purified using the QIAprep Spin Miniprep Kit (27,104; Qiagen, Germany). The correct insertion of the fragment into the vector was verified by submitting

purified plasmid for sequencing (Genewiz Inc., NJ). Resultant sequence data verification and alignment were performed on Seaview version 4.6 (Galtier et al. 1996; Gouy et al. 2010).

P. tricornutum genetic transformation and selection of transformants

pKS-ShBle-Phatr3_EG02570-FA vector (5 µg) was coated onto M17 tungsten particles (1.1 µm) according to the manufacturer's instructions (Bio-Rad). Approximately 5×10^7 wild-type *P. tricornutum* cells were plated on 1% agar plates (50% F/2) and incubated for one day before the transformation. The cells were bombarded with the DNA-coated M17 particles at 1,550 psi (Falciatore et al. 1999) using a PDS-1000/ He Particle Delivery System (Bio-Rad, CA). The plates were incubated at 100 µmol photons m^{-2} s^{-1} constant illumination at 18 °C for 48 h to recover. Cells were then replated onto selective 1% agar plates (50% F/2) with 100 µg/mL Zeocin™. Plates were incubated at 40 µmol photons m^{-2} s^{-1} for 3–4 weeks to enable the transformed clones to grow. The transformation event yielded 63 colonies. To screen for putative knockdown strains, each culture was propagated in liquid F/2 supplemented with Zeocin and then split into two cultures—one grown under constant high light (HL) conditions of ~ 750–800 µmol photons m^{-2} s^{-1} and one under constant low light (LL) conditions of 15–25 µmol photons m^{-2} s^{-1}. They were then screened for abnormal LL/HL ratios of Chl a /cell of each line, using pigment fluorescent data acquired with the Guava® easyCyte™ 12 HT Sampling Flow Cytometer (0500–4012; EMD Millipore Sigma, MA). Of these, six were identified as showing most significantly variable phenotypes (Supplemental Table S5), and the transformant line with the most stable phenotype, was selected for further characterization.

Quantification of target gene mRNA copies using quantitative real-time PCR (RT-qPCR)

Samples for RT-qPCR were pelleted by centrifuging 6×10^7 cells for 5 min at 6500×*g* at 4 °C. The samples were frozen in liquid N_2 and stored at − 80 °C. Total RNA was extracted using TRIzol™ Reagent (15596026, ThermoFisher Scientific; MA), followed by cleaning with RNeasy MinElute Kit (74204; Qiagen, Germany). DNA contamination was removed using Ambion Turbo DNase (AM1907; Life Technologies, CA). Samples were run on an RNAse-free polyacrylamide gel to confirm RNA integrity. Total RNA quantification and quality assessment were made spectrophotometrically on a DS-11 FX + Series Spectrophotometer/ Fluorometer (DS-11 FX, DeNovix Inc.; DE). Double-stranded cDNA was generated using random primers with a High-Capacity cDNA Reverse Transcription Kit (4368814, ThermoFisher Scientific; MA) and directly used as the template for qPCR. The housekeeping gene used as a reference was the small sub-unit of RNA polymerase (RPS). Primers for target genes (Supplemental Table S4) were designed with Primer Express™ Software v3.0.1 (4363991, ThermoFisher Scientific; MA). The area for qPCR amplification was a 57 bp amplicon 143 bp downstream of the RNA silencing construct binding site. The PCR reaction was performed using the Applied Biosystems Power SYBR® Green Master Mix (4309155; Life Technologies, CA) on a QuantStudio3 (A28136; Applied Biosystems, CA). A serial dilution of five orders of magnitude of WT genomic DNA was used to plot a standard curve for copy number calculation with each primer pair. All standard curves had an $R^2 > 0.94$.

Gene identification

To identify the transcriptional regulators responsible for the differential expression of these genes, the sequence of the promoter regions of the characterized *lhc*s were analyzed for putative transcription factor binding sites (TFBS), using MatInspector (Release 8.1). The matrix library (version 9.1) of the Genomatix promoter database contained 1424 matrices in 418 families classified into fungi, insects, plats, vertebrates, miscellaneous and general core promoter elements. For our purposes, the databases for fungi (binding site descriptions of 140 TF's), plants (binding site descriptions of 1160 TF's from several plants species), miscellaneous and general core promoter elements were selected (www.genomatix.de/). MatInspector scans the query nucleotide sequences for matches by calculating a matrix similarity score. Only if the test sequence has the most conserved nucleotide at each position of the matrix, does the similarity score reach 1 (Cartharius et al. 2005). Thirty-one different transcription factor family-types were identified as having binding potential to the promoter regions of the 34 *lhc* gene queries (Table 1; Supplemental Table S1). All characterized *lhc* genes had at least one or more binding sites for the TF's belonging to the MYB-like protein family.

Analytical methods

Cell densities were determined using a Beckman Multisizer™ 3 Coulter Counter® (6605697; Beckman Coulter Life Sciences, IN) as well as a Guava® easyCyte™ 12 HT Sampling Flow Cytometer (0500-4012; EMD Millipore Sigma, MA). Relative chlorophyll fluorescence data obtained on the Guava were used for high throughput screening.

Cellular Chlorophyll a (Chl *a*) was measured spectrophotometrically on a Cary 60 UV–Vis Spectrophotometer (Agilent Technologies, CA) extracted in 90% acetone (Jeffrey and Humphrey 1975) in a FastPrep-24™ using Lysis

Table 1 The various transcription factor binding sites (TFBS) predicted to be present in the upstream regulatory regions of the 34 characterized *lhc* genes in *P. tricornutum*

Transcription binding factor family	# of lhc genes having TFB sites	*p* value
MYB-like proteins	34	0.039
Motifs of plastid response elements	20	0.045
Coupling element 3 sequence	16	0.034
General transcription factor IID, GTF2D	15	0.019
ER stress-response elements	13	0.027
LFY binding site	13	0.043
Auxin response element	11	0.032
Octamer motif of Histone H3, H4 promoters	11	0.034
E2F-homolog cell cycle regulators	8	0.039
Salt-/drought-responsive elements	8	0.047
Sulphur limitation elements	8	0.025
VIP1 responsive elements	8	0.025
General transcription factor IIIC, GTF3C	7	0.002
Arabidopsis CDC5 homolog	7	0.013
Nodulin consensus sequence 3	7	0.011
Plant GATA-type zinc finger protein	6	0.039
Dc3 promoter binding factors	6	0.018
GCC box family	6	0.023
Plant nitrate-responsive cis-elements	6	0.013
5′-part of bipartite RAV1 binding site	6	0.024
Soybean embryo factor 3	6	0.028
TALE (3-aa acid loop extension) class homeodomain proteins	6	0.007
Yeast TATA binding protein factor	5	0.022
Fungal and oomycete pathogen response cluster—promoter motif	5	0.029
Activation of the arbuscular mycorrhizal (AM)-mediated inorganic phosphate transporter genes	5	0.016
Upstream sequence element of U-snRNA genes	5	0.020
EPF-type zinc finger factors	4	0.016
Conserved box A in PAL and 4CL gene promoters	4	0.013
Soybean embryo factor 4	3	0.030
Iron-dependent regulatory sequences	2	0.006
RNA polymerase II transcription factor II B	1	0.010

Matrix C with modifications to manufacturer's instructions (116005500, 6912-100; MP Biomedicals; CA). In vivo absorption spectra were measured with an SLM-Aminco DW-2000 spectrophotometer (Olis; GA) using optically thin cell suspensions. These values were normalized to Chl *a* and used to calculate the optical absorption cross-sections, referred to as *a** (Falkowski et al. 1985; Dubinsky et al. 1986).

PSII biophysical characteristics were measured on a custom-built fluorescence induction and relaxation instrument (FIRe, Satlantic Inc., Canada; Gorbunov and Falkowski 2004). The kinetics of the single-turnover saturating flash were analyzed to obtain the maximum quantum efficiency of photochemistry (F_V/F_M) and the functional absorption cross-section of PSII (σ_{PSII}) (Gorbunov and Falkowski 2004).

Functional metabolic assignment was determined using Ensembl for Phatr3_EG02570 (protists.ensembl.org/Phaeodactylum_tricornutum), and the NCBI database (www.ncbi.nlm.nih.gov). HECTAR v1.3 software was used to predict subcellular targeting for heterokont proteins (webtools.sb-roscoff.fr); TMHMM was used to predict transmembrane helices in proteins (www.cbs.dtu.dk/services/TMHMM); Signal P 4.0 Server was used to predict presence and location of signal peptide cleavage sites (www.cbs.dtu.dk/services/SignalP); and Target P1.1 Server was used to predict the subcellular location of eukaryotic proteins (www.cbs.dtu.dk/services/TargetP).

Protein expression, extraction, verification

For high-efficiency protein expression, Phatr3_EG02570 was codon-optimized for *E. coli* with an additional 6-HisTag at the carboxyl terminal, in between *Nde*I and *Xho*I sites and custom synthesized by Genewiz Inc. This synthetic DNA template was ligated into a pET30b expression vector (Supplemental Plasmid Map S2), transformed into One Shot™ BL21(DE3)pLysE Chemically Competent *E. coli* (C656503, Invitrogen™, MA), to overexpress this 6xHis-tagged-MYB protein. 200 mL LB broth with 50 µg/mL Kanamycin inoculated cultures were grown at 37 °C at 200 rpm, induced with 1 mM Isopropyl-β-D-thiogalactopyranoside (IPTG; I2481, Gold Biotechnology®, MO) at 20 °C overnight. Soluble and insoluble fractions of the resultant pelleted cells were extracted using the pET System Manual (10th edition) and visualized on a 4–10% agarose Bio-rad Mini-Protean TGX stain-free pre-cast SDS-PAGE gel, with a Biorad Dual Precision Plus Protein™ Dual Color Standard (#1610374, Bio-Rad, CA). Western blot was carried out using a Trans-Blot Turbo™ Transfer System Transfer Pack following manufacturer's protocol (Bio-Rad). Incubation with Histidine (C-term) tag (6xHis) mouse monoclonal primary antibody (#R930-25, Invitrogen, MA) and anti-mouse IgG (whole molecule)—alkaline phosphatase, rRabbit secondary antibody (A2418, Sigma-Aldrich, MA) was conducted to detect the His-tagged recombinant protein of interest with colorimetric reactions with 5-bromo-4-chloro-3-indolyl phosphate disodium salt (BCIP) and nitrotetrazolium-blue chloride (NBT). For purification of the IPTG overexpressed protein, cell pellets were resuspended in equilibration buffer (as per manufacturer's instructions) for HisPur™ Ni–NTA Resin (88221, ThermoScientific, MA) and lysed with CelLytic™ Express (C1990, Millipore Sigma, MA) according to manufacturer's protocol. The whole cell lysate was fractionated on the Ni–NTA column using manufacturer-supplied protocol. Protein fraction eluted by an additional 100 mM imidazole elution step, was concentrated using an Amicon Ultra 0.5 mL (C82301, Millipore Sigma, MA) and used in protein-DNA assay as the 'Ligand'.

Protein-DNA interaction: BLItz® assay

Of the 143 potential MYB-binding sites in the *lhc* gene regulatory regions, nine sites were selected from the most differentially expressed LHC's under LL, as well as to represent one of each type of the MYB binding sites identified (Table S2). These 23-base long Oligo-DNA fragments were synthesized (Integrated DNA Technologies, USA) (Table S3) and used as 'analytes'.

Multiple negative controls were prepared by shearing the target DNA as well as double-stranded DNA at room temperature and high heat-shocking temperatures. Intact DNA, amplified from unrelated regions of *P. tricornutum* genome with no sequence complementarity with the protein probes, were also tested. Bio-layer interferometry was carried out on BLItz® label-free protein analysis platform (45-5000, ForteBio/Sartorius, Germany) using Dip and Read nickel-nitrilotriacetic acid (NTA) biosensors (18-5101, Sartorius, Germany) to bind 286 µg/mL of the tagged ligand. Kinetics of binding were measured with varying concentration of analyte (10–800 nM of DNA) and analyzed by BLItz® Pro Software.

Results

Effect of light on chlorophyll pigment accumulation

Cells were fully acclimated to low light intensity of 20 µmol photons m^{-2} s^{-1} (LL) and high light intensity of 940 µmol photons m^{-2} s^{-1} (HL). A decrease in light in the growth of the cells lead to a threefold increase in chlorophyll a content of wild-type (WT) *P. tricornutum* cells (Fig. 1).

Transcription factor binding site (TFBS) prediction

To identify the transcriptional regulators responsible for the differential expression of these genes, the sequence of the promoter regions of the characterized *lhc*'s were analyzed for putative transcription factor binding sites (TFBS), using MatInspector (Release 8.1). The matrix library (version 9.1) of the Genomatix promoter database contained 1424 matrices in 418 families classified into fungi, insects, plants, vertebrates, miscellaneous

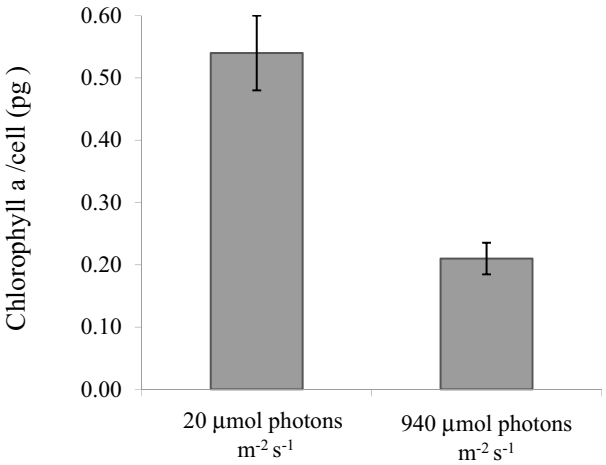

Fig. 1 Chlorophyll *a* content per cell of Wild-type *P. tricornutum* cultures fully acclimated to low light 20 µmol photons m^{-2} s^{-1} (left) and high light 940 µmol photons m^{-2} s^{-1} (right) ($n = 3$; Error bars represent ± SD)

and general core promoter elements. For our purposes, the databases for fungi (binding site descriptions of 140 TF's), plants (binding site descriptions of 1160 TF's from several plants species), miscellaneous and general core promoter elements were selected (www.genomatix.de/). MatInspector scans the query nucleotide sequences for matches by calculating a matrix similarity score. Only if the test sequence has the most conserved nucleotide at each position of the matrix, does the similarity score reach 1 (Cartharius et al. 2005). 31 different transcription factor family-types were identified as having binding potential to the promoter regions of the 34 *lhc* gene queries (Table 1; Supplemental Table S1). All characterized *lhc* genes had at least one or more binding sites for the TF's belonging to the MYB-like protein family.

Consensus sequence determination

Over one hundred Myb-predicted genomic sequences in the region from -200 to -1 relative to the transcription start or the end of the upstream coding region, from the promoter regions of 34 *lhc* genes were examined. The MatInspector software identified all the predicted Myb TFBS's, and their similarity to nine different Myb-type families (Supplemental Table S2). Consensus sequences of each type of Myb-family binding site were also identified. These motif graphics were constructed by WebLogo (http://weblogo.berkeley.edu), where the size of each letter is proportional to the frequency of occurrence of each of those nucleotides in that position (Fig. 2). In fact, the promoter region of each gene was predicted to have between 2 to 15 potential MYB-binding sites, which were found to exist on either the sense or antisense strand (Supplemental Table S2).

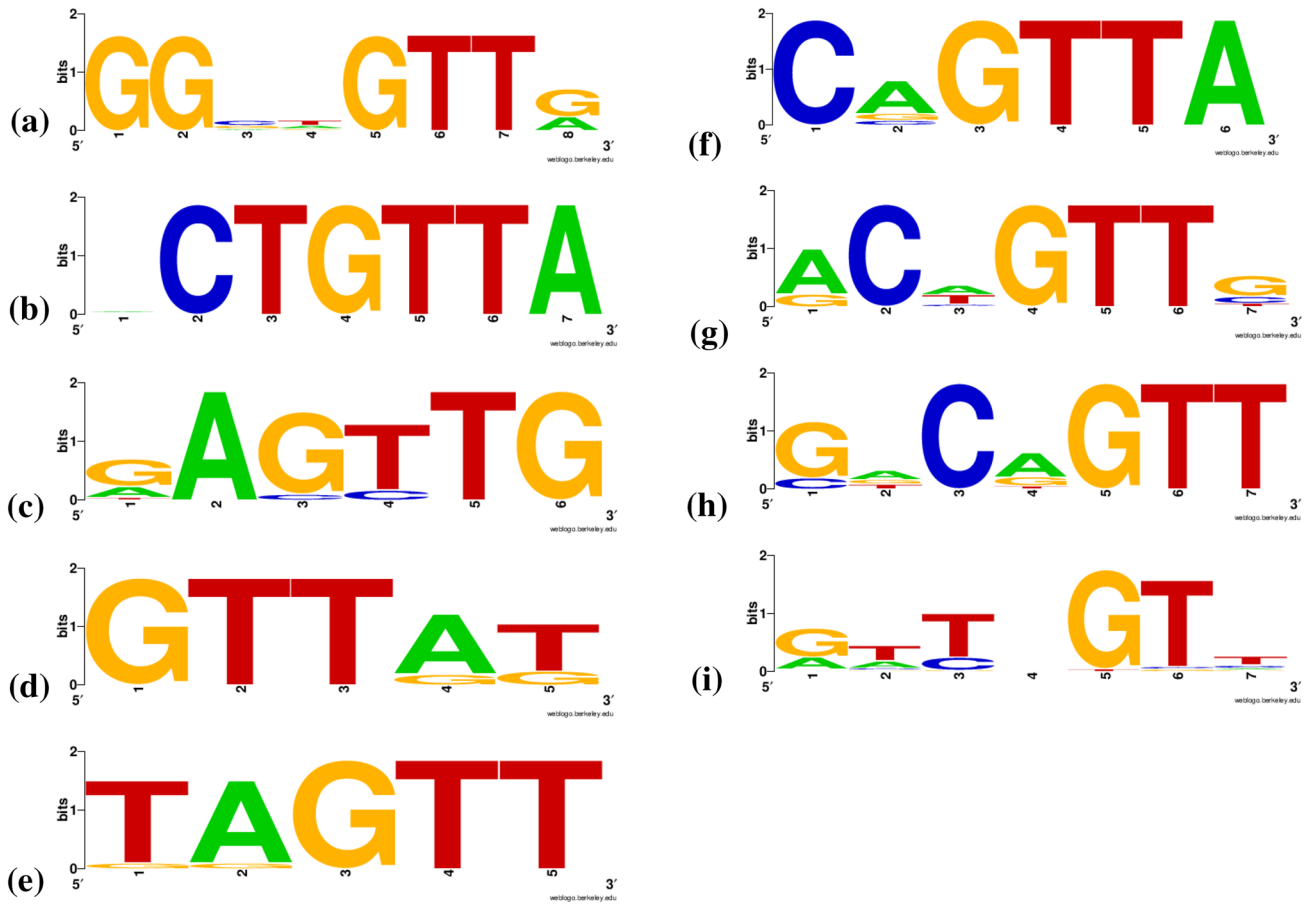

Fig. 2 The consensus binding motifs for 143 DNA-binding sites (categorized into nine different Myb-types by MatInspector) in the promoter regions of *P.tricornutum*'s *lhc* genes. Here are the motifs constructed by Weblogo, where the height of the letter is indicative of the relative frequency of occurrence of that nucleotide. **a** Anther-specific myb gene from tobacco (*6 TFB seqs*); **b** AS1/AS2 repressor complex binding motif -I (*18 TFB seqs*); **c** CAACTC regulatory elements, GA-inducible (*15 TFB seqs*); **d** GA-regulated myb gene from barley (*13 TFB seqs*); **e** Myb domain protein 96 (MYBCOV1) (*15 TFB seqs*); **f** Myb domain protein r1 (ATMYB44) (*19 TFB seqs*); **g** Myb-domain transcription factor werewolf (*9 TFB seqs*); **h** R2R3-type myb-like transcription factor (*12 TFB seqs*); **i** Myb-like protein of Petunia hybrida (*36 TFB seqs*)

Identification of photoacclimation MYB

With this established relevance of one or more MYB-like TFs as a regulator of *lhc* gene expression in *P. tricornutum*, a search for MYB genes involved in photoacclimation of unicellular photoautotrophs was conducted. A mutation in an ORF in the *Nannochloropsis gaditana* genome (Nangad1|scaffold _1:565183-567446), which has a MYB-like DNA-binding motif, resulted in a locked in high light-acclimated phenotype, indicating a critical role for this TF in light intensity photoacclimation in this organism (Bailey. 2014. US Patent 2014/0220638). A BLAST search of this hypothetical protein revealed that orthologs of this gene were present in the genome of *P. tricornutum* as Phatr3_EG02570 and its duplicate EG01922. In silico analysis of these two hypothetical proteins revealed a conserved domain for a MYB-like DNA-binding transcription factor. These genes were not identified by Rayko et al. 2010. The absence of any signal or plastid targeted peptides as well as trans- or membrane-associated domains (in silico sequence-based predictions), suggests that this protein is likely a soluble nuclear transcription factor (Table 2). In fact, our transcriptome shows a 2.5- to 3.5-fold increase in gene expression of these MYB genes in LL as compared to HL (Table 2; NCBI GEO Accession # GSE133301).

Phenotypic characterization of transformant strain shows disruption in the photoacclimation response

To examine its potential role in photoacclimation, this gene was targeted by an antisense RNAi. Out of the 63 resultant RNAi transformant lines, 41 strains showed more than 25% increase/decrease in chlorophyll pigment accumulation in the cell. Given that we were interested in how this diatom acclimates to LL, we selected a strain in which this process was interrupted, i.e. a strain that was incapable of accumulating expected quantities of light harvesting pigments in response to LL growth environments. The phenotype of the most stable Phatr3_EG02570 (LHC-regulating MYB or LRM) transformant line #47 (LRM-47) was selected.

LRM-47 grown in HL (750–800 µmols photons m^{-2} s^{-1}) showed a ~ 70% increase in MYB transcript accumulation (Table 3). HL acclimated cells of this transformant line showed reduced growth rate of ~ 70% of WT, 3.5- to fourfold higher chlorophyll accumulation, which consequently decreased the optical cross-section a^*. An insignificant decrease in F_v/F_m might indicate a slight decline in

Table 2 RNA-Seq differential expression of MYB-genes of interest in low light acclimated cells as compared to high light, as well as in silico sequence-based predictions of phenotype

Gene number (Phatr3)	Log2 fold-change LL vs. HL	Fold-change in LL vs. HL	BLAST Hit	NCBI conserved protein domains	Presence of signal peptide	Trans-membrane	Anchored to membrane	Targeted to plastid
EG02570	1.36	2.56	Predicted protein	MYB-like DNA-binding transcription factor	–	–	–	–
EG01922	1.84	3.58	Predicted protein	MYB-like DNA-binding transcription factor	–	–	–	–

Phatr3—gene identification numbers from third annotation of genome (protists.ensembl.org); LL—low light intensity of 20 µmol photons m^{-2} s^{-1}; HL—high light intensity of 940 µmol photons m^{-2} s^{-1}; NCBI—The National Center for Biotechnology Information database; BLAST Hit—Results from The Basic Local Alignment Search Tool of NCBI; (+) indicates presence; (−) indicates absence. ($n = 3$; $p < 0.05$)

Table 3 Phenotypic characterization of transformant strain LRM-47 targeting MYB domain of Phatr3_EG02570/EG01922. (n = at least 3; $p < 0.05$; ± SD)

	WT (HL)	LRM-47 (HL)	WT (LL)	LRM-47 (LL)
Exponential growth rate (µ day^{-1})	1.1 ± 0.1	0.72 ± 0.5	0.49 ± 0.04	1.33 ± 0.3
Chlorophyll *a* content per cell (pg)	0.27 ± 0.1	1.0 ± 0.4	0.42 ± 0.1	0.43 ± 0.1
Optical cross-section a^* (m^2/mg *Chl a*)	41.1 ± 3.5	8.7 ± 2.8	28.6 ± 1.4	39.8 ± 3.0
Functional cross-section of PSII σ_{PSII} ($Å^2$)	364 ± 48	353 ± 47	557 ± 22	563 ± 33
Quantum efficiency of photochemistry (F_v/F_m)	0.53 ± 0.03	0.49 ± 0.02	0.56 ± 0.01	0.55 ± 0.02
Electron transport rate through PSII (e^-/s per RC)	1362 ± 204	1960 ± 89	1259 ± 169	1319 ± 88
qRT-PCR (normalized to WT HL)	1 ± n/a	1.72 ± 0.42	1.96 ± 0.59	1.70 ± 1.09

HL is 750–800 µmols photons m^{-2} s^{-1}; LL is 20 µmols photons m^{-2} s^{-1}

the quantum yield of PSII photochemistry. A 44% increase in the rate at which electrons are transported through PSII gives information on the state of the PET components. There was a 35% decrease in MYB transcript levels observed in LL acclimated LRM-47 cells, which concurrently showed a more than twofold increase in growth rate accompanied by a marginal increase in a^* (characteristic of a decline in antenna pigment accumulation and thylakoid packaging), despite there not being any change in chlorophyll content. No significant difference was observed in any of the other parameters, as compared to the WT grown under the same conditions.

Recombinant protein overexpression, extraction and purification

To investigate this potential Myb-*lhc* gene interaction, a C-terminal 6His-tagged recombinant LRM protein was expressed by IPTG induced BL21(DE3)pLysE *E.coli* cells (Supplementary Plasmid Map S2). SDS-PAGE gels of the soluble and insoluble fractions of uninduced (control) and induced (1 mM IPTG) cells revealed that a distinct band is present in the insoluble fraction of the induced culture at about 65–76 kDa size (Fig. 3a). Given that the in silico estimation of the protein weight based on amino acid composition was 55.5 kDa, it is very likely that the difference in size is likely due to aggregation. To verify that this is indeed our recombinant protein, a western blot with a His-specific primary antibody was performed. This analysis revealed that the only clear band containing His-tagged proteins, and therefore the protein of interest, is ~ 65 to 75 *kDa* (Fig. 3b). With this confirmation, we overexpressed and purified the protein in a Ni–NTA column, to be used for further assays.

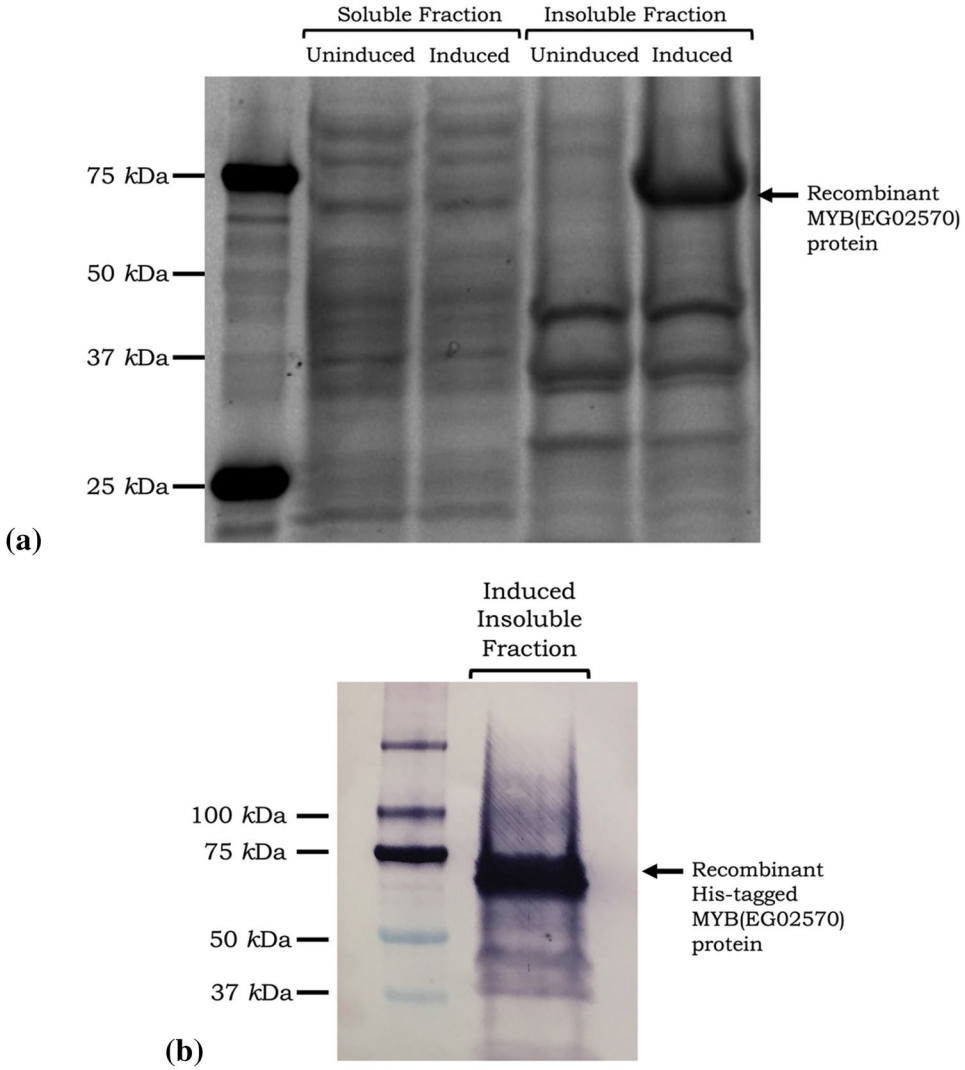

Fig. 3 **a** SDS-PAGE gel of soluble and insoluble fractions of uninduced (control) and 1 mM IPTG induced pET30b-MYB(EG02570). The band present at ~ 65 to 75 kDA in the induced insoluble fraction is the recombinant protein of interest. **b** Chromogenic alkaline phosphatase Western blot of the insoluble fraction of induced cells to confirm that the band observed at ~ 65–75 kDa is the His-tagged protein of interest

Bio-layer interferometry protein-DNA interaction determination and kinetics

The quantitative binding of MYB (EG02570) with sites upstream of the *lhc* genes was investigated using the biolayer interferometry mechanism (BLI) with the BLItz® instrument. Here, the DNA is allowed to interact with the protein immobilized on the optical biosensor tip, and the resultant binding increases optical thickness. The light reflected from the tip of the bound or unbound DNA–protein layer, results in a distinguishable wavelength shift that can be detected and measured in real time (Abdiche et al. 2008; Nguyen et al. 2007; Di et al. 2016; Desai et al. 2018).

All the negative controls including denatured-sheared double-stranded DNA which was not included in Table 4, resulted in the exact same unspecific values for K_D and k_d, along with incomplete binding sensograms, confirming zero binding. The kinetics of different concentrations (between 10 and 800 nM) of each analyte were measured with a constant concentration of the ligand. All the pre-LHC regions selected as analytes showed similar association kinetics with the MYB ligand (Table 4). With the exception of the negative control which was a non-Myb section of DNA in the regulatory region of *lhc*F8, no more than a threefold difference in k_a values was observed between analytes. The same trend was observed for the dissociation kinetics, except that they were an order of magnitude lower. This means that while the promoter regions of these DNAs associate quickly with our protein of interest, the binding does not last long and that dissociation occurs at a much faster rate as compared to the association. The dissociation equilibrium constants were all in the millimolar range (as opposed to known regulators which are in the micromolar range), indicating similar rates of binding with all the tested analytes.

Discussion

The results of this study reveal, for the first time, that Myb-type transcription factors are involved in the retrograde expression of *lhc* genes in a marine diatom.

The terminal component of any retrograde signaling cascade would have to be a nuclear TF protein with a DNA-binding motif. To identify the TF or regulatory molecule that could change the expression of more than one *lhc* gene in response to a stimulus, the sequences of their promoter regions were examined. This genetic analysis revealed 143 binding sites for potential MYB-like TFs, dispersed between the promoter regions of every *lhc* in *P. tricornutum* (Supplemental Table S2). Interfering with the functional capability of that TF would result in a discontinuation of the signaling cascade. The resultant cells would lose the ability to correctly adjust the expression of their *lhc* genes, in response to changes in light intensity. One such TF was identified in the green alga *Nannochloropsis gaditana*, where a mutation in a hypothetical protein with a predicted MYB-like functional

Table 4 Protein—DNA interaction assay using BLItz® platform was performed with 5174 nM purified pET30b-MYB-6XHis protein or Ligand, attached to Ni–NTA biosensors, and oligo fragments of MYB-binding site upstream of the indicated *lhc* genes

Analyte	*n*	K_D (M)	k_a (1/Ms)	k_d (1/s)
pre-F5	3	$(2.7 \pm 0.7) \times 10^{-2}$ *p = 0.055*	4.8 ± 1.6 *p = 0.068*	0.13 ± 0.6 *p = 0.055*
pre-F8	3	$(2.5 \pm 1.2) \times 10^{-2}$ *p = 0.066*	1.7 ± 0.3 *p = 0.069*	0.04 ± 0.02 *p = 0.066*
pre-F15	4	$(2.6 \pm 1.0) \times 10^{-2}$ *p = 0.026*	4.6 ± 1.8 *p = 0.027*	0.13 ± 0.07 *p = 0.027*
pre-R10	3	$(2.3 \pm 1.2) \times 10^{-2}$ *p = 0.055*	2.8 ± 1.4 *p = 0.062*	0.05 ± 0.00 *p = 0.055*
pre-X1	4	$(1.4 \pm 0.5) \times 10^{-2}$ *p = 0.087*	5.1 ± 0.7 *p = 0.102*	0.11 ± 0.03 *p = 0.088*
pre-X2	4	$(1.4 \pm 0.5) \times 10^{-2}$ *p = 0.083*	3.2 ± 1.4 *p = 0.089*	0.12 ± 0.12 *p = 0.088*
Neg. Controls	3	$< (1.0 \pm 0.0) \times 10^{-12}$ *p = n/a*	$(4.3 \pm 0.9) \times 10 + ^{5}$ *p = 0.0008*	$< (1.0 \pm 0.0) \times 10^{-7}$ *p = n/a*

Kinetic parameter values (averages ± SD) were generated by the BLItz® Pro software

Analytes indicate the pre-specified LHC gene upstream region that was used to test binding

K_D which is k_d divided by k_a (disassociation equilibrium constant), is defined as the concentration at which 50% of ligand binding sites are occupied by the analyte

k_a (association rate constant) is defined as the number of complexes formed per second in a 1 Molar solution of ligand and analyte (1/Ms)

k_d (disassociation rate constant) is defined as the number of complexes that decay per second (1/s)

n, number of experimental repeats

P values were calculated using Student's *t*-test (2-tailed)

domain resulted in cells that displayed HL acclimated phenotypes (growth, pigment accumulation, NPQ capabilities, PET characteristics, etc.), irrespective of the incident light intensity in their environment (Bailey, S. 2014. US Patent 2014/0220638). By eliminating the binding capability of this particular TF, the algae lost the ability to successfully translate the environmental signals into genetic modifications that result in photophysiological responses.

The identification of a TF ortholog in the Eustimatophyte *Nanochloropsis gaditana* in distantly related diatom, *P. tricornutum* stongly suggests this protein plays a similar role in regulating the expression of LHC genes. Inducing changes in transcript levels of the hypothetical MYB, hereafter referred to as LHC-Regulating-MYB (LRM), resulted in a strain that could not acclimate to high light. Cells with a higher than normal accumulation of LRM transcripts when grown in HL (Table 3) synthesized more light LHCs, which increased the packaging of thylakoid membranes in the plastid (Berner et al. 1989). Along with lower growth rates, this transformant clearly displayed characteristic phenotypes of WT cells acclimated to LL. The increased rate at which electrons are transported on the acceptor side of PSII in the LRM-47 transformant strain indicates a more oxidized PQ pool than in the HL WT (HL). When acclimated to LL, the LRM-47 showed a decrease in LRM transcript accumulation, and some HL acclimated traits such as higher growth rate, a slight increase in PSII electron transport rate as well as a slight decrease in thylakoid packaging, despite no obvious change in chlorophyll content. Table 2 shows that under LL, WT cells produced 1.4- to 2.6-fold more of the LRM transcript than under HL growth. When the antisense transformants accumulated more LRM, the HL acclimated cells clearly behaved like LL cells, and when the LL transformants accumulated HL levels of LRM, they displayed some WT HL phenotypes. Additionally, minimal differences in LRM between LL and HL fully acclimated cells suggest that this TF is constitutively expressed to keep the cell in a poised state, to be able to rapidly respond to changes in light intensity. We therefore propose that this TF possibly binds to, and regulates, the expression of one or more *lhc* genes in *P. tricornutum*, and is a critical retrograde signal.

In conclusion, this paper provides compelling evidence that an Myb-type LRM transcription factor binds to one or more *lhc* genes. We propose that LRM is a coactivator of *lhc* gene transcription, that is upregulated in LL to stimulate an increase in the biosynthesis and accumulation of light harvesting complexes that are needed to increase the efficiency of photon capture. The phenotype of this cell has significantly higher growth rates at low light relative to the wild type (Table 3), suggesting this type of transformation may lead to higher algal yields in mass production at high cell densities. As light intensity increases, however, the enlarged resultant optical cross section of the antenna would facilitate photo-oxidative damage. Therefore, reducing synthesis of this LRM TF would alleviate transcriptional pressure on the *lhc*'s, resulting in their downregulation as required for acclimation to high growth irradiance.

Supplementary Information The online version contains supplementary material available at https://doi.org/10.1007/s11120-022-00915-w.

Acknowledgements We thank Ehud Zelzion and Nicole Wagner (Rutgers, The State University of New Jersey) for the transcriptome sequencing and its analysis and to Shaun Bailey and Orly Levitan for discussions. This work, in its entirety, was included in the thesis of Agarwal A. (2021), titled "Inter-organellar signaling in a diatom" (Rutgers University 2021).

Author contributions AA and RD designed research. AA and RD performed research. AA, RD and PGF analyzed data. AA wrote first draft of manuscript. All authors contributed to manuscript revision, read, and approved the submitted version.

Funding This research was supported by the Rutgers University Professional Development Fund, the James G. Gibson (Biodiesel) Fund to PGF, and the Bennett L. Smith Endowment in Business and Natural Resources at Rutgers University to PGF.

Declarations

Conflict of interest The authors declare no conflict of interest.

References

Abdiche Y, Malashock D, Pinkerton A, Pons J (2008) Determining kinetics and affinities of protein interactions using a parallel real-time label-free biosensor, the octet. Anal Biochem 377(2):209–217. https://doi.org/10.1016/j.ab.2008.03.035

Agarwal A (2021) Inter-organellar signaling in a diatom. 0–181. https://doi.org/10.7282/T3-27SQ-E338.

Albert NW, Lewis DH, Zhang H, Irving LJ, Jameson PE, Davies KM (2009) Light-induced vegetative anthocyanin pigmentation in petunia. J Exp Bot. https://doi.org/10.1093/jxb/erp097

Bailey S, McCarren J, Lieberman SL, Meuser JE, Romano AE, Yee LSD, Brown RC et al (2013) Algal mutants having a locked-in high light acclimated phenoptype. US 2014/0220638 Al, issued 2013

Ballesteros ML, Bolle C, Lois LM, Moore JM, Vielle-Calzada JP, Grossniklaus U, Chua NH (2001) LAF1, a MYB transcription activator for Phytochrome A signaling. Genes Dev. https://doi.org/10.1101/gad.915001

Berner T, Dubinsky Z, Wyman K, Falkowski PG (1989) Photoadaptation and the 'Package' effect in *Dunaliella tertiolecta* (Chlorophyceae) 1. J Phycol 25(1):70–78. https://doi.org/10.1111/J.0022-3646.1989.00070.X

Büchel C (2019) Light harvesting complexes in chlorophyll c-containing algae. Biochim Biophys Acta Bioenergy 1861:148027

Buck JM, Sherman J, Bártulos CR, Serif M, Halder M, Henkel J, Falciatore A et al (2019) Lhcx proteins provide photoprotection via thermal dissipation of absorbed light in the diatom *Phaeodactylum tricornutum*. Nat Commun 10(1):1–12. https://doi.org/10.1038/s41467-019-12043-6

Cartharius K, Frech K, Grote K, Klocke B, Haltmeier M, Klingenhoff A, Frisch M, Bayerlein M, Werner T (2005) MatInspector and

beyond: promoter analysis based on transcription factor binding sites. Bioinformatics 21(13):2933–2942. https://doi.org/10.1093/bioinformatics/bti473

Churin Y, Adam E, Kozma-Bognar L, Nagy F, Börner T (2003) Characterization of two Myb-like transcription factors binding to CAB promoters in wheat and barley. Plant Mol Biol. https://doi.org/10.1023/A:1023934232662

De Martino A, Meichenin A, Shi J, Pan K, Bowler C (2007) Genetic and phenotypic characterization of *Phaeodactylum tricornutum* (Bacillariophyceae) accessions 1. J Phycol 43(5):992–1009. https://doi.org/10.1111/j.1529-8817.2007.00384.x

Desai M, Wurihan W, Di R, Fondell JD, Nickels BE, Bao X, Fan H (2018) Role for GrgA in regulation of 28-dependent transcription in the obligate intracellular bacterial pathogen chlamydia trachomatis. J Bacteriol. https://doi.org/10.1128/JB.00298-18

Di R, Huang Q, Stulberg M, Zhao L, Levy L (2016) Detection of plant quarantine pathogen *Ralstonia solanacearum* race 3 biovar 2 with portable POCKIT™ and BLItz® systems. J Plant Health 1(1):103–111

Dinamarca J, Levitan O, Kenchappa Kumaraswamy G, Lun DS, Falkowski PG (2017) Overexpression of a diacylglycerol acyltransferase gene in *Phaeodactylum tricornutum* directs carbon towards lipid biosynthesis. J Phycol 53(2):405–414. https://doi.org/10.1111/jpy.12513

Dubinsky Z, Falkowski PG, Wyman K (1986) Light harvesting and utilization by phytoplankton. Plant Cell Physiol 27(7):1335–1349

Durnford DG, Falkowski PG (1997) Chloroplast redox regulation of nuclear gene transcription during photoacclimation. Photosynth Res 53(2–3):229–241. https://doi.org/10.1023/a:1005815725371

Escoubas JM, Lomas M, LaRoche J, Falkowski PG (1995) Light intensity regulation of cab gene transcription is signaled by the redox state of the plastoquinone pool. Proc Natl Acad Sci 92(22):10237–10241. https://doi.org/10.1073/pnas.92.22.10237

Falciatore A, Casotti R, Leblanc C, Abrescia C, Bowler C (1999) Transformation of nonselectable reporter genes in marine diatoms. Mar Biotechnol 1(3):239–251. https://doi.org/10.1007/PL00011773

Falkowski PG, LaRoche J (1991) Acclimation to spectral irradiance in algae. J Phycol. https://doi.org/10.1111/j.0022-3646.1991.00008.x

Falkowski PG, Dubinsky Z, Wyman K (1985) Growth-irradiance relationships in phytoplankton. Limnol Oceanogr 30(2):311–321. https://doi.org/10.4319/lo.1985.30.2.0311

Falkowski PG, Katz ME, Knoll AH, Quigg A, Raven JA, Schofield O, Taylor FJR (2004) The Evolution of Modern Eukaryotic Phytoplankton. Science. https://doi.org/10.1126/science.1095964

Galtier N, Gouy M, Gautier C (1996) Seaview and Phylo_Win: two graphic tools for sequence alignment and molecular phylogeny. Bioinformatics 12(6):543–548. https://doi.org/10.1093/bioinformatics/12.6.543

Gibson DG, Young L, Chuang RY, Craig Venter J, Hutchison CA, Smith HO (2009) Enzymatic assembly of DNA molecules up to several hundred kilobases. Nat Methods 6(5):343–345. https://doi.org/10.1038/nmeth.1318

Gibson DG, Glass JI, Lartigue C, Noskov VN, Chuang R-Y, Algire MA, Benders GA et al (2010) Creation of a bacterial cell controlled by a chemically synthesized genome. Science 329(5987):52–56. https://doi.org/10.1126/science.1190719

Glatz A, Vass I, Los DA, Vigh L (1999) The synechocystis model of stress: from molecular chaperones to membranes. Plant Physiol Biochem. https://doi.org/10.1016/S0981-9428(99)80061-8

Goldman JC, McCarthy JJ (1978) Steady state growth and ammonium uptake of a fast-growing marine diatom. Limnol Oceanogr 23(4):695–703. https://doi.org/10.4319/lo.1978.23.4.0695

Gorbunov MY, Falkowski PG (2004) Fluorescence induction and relaxation (FIRe) technique and instrumentation for monitoring photosynthetic processes and primary production in aquatic ecosystems. In: Photosynthesis: fundamental aspects to global perspectives-proceedings of the 13th international congress of photosynthesis

Gouy M, Guindon S, Gascuel O (2010) Sea View Version 4: a multiplatform graphical user interface for sequence alignment and phylogenetic tree building. Mol Biol Evol 27(2):221–224. https://doi.org/10.1093/molbev/msp259

Grossman AR (2000) Chlamydomonas reinhardtii and photosynthesis: genetics to genomics. Curr Opin Plant Biol. https://doi.org/10.1016/S1369-5266(99)00053-9

Guillard RRL, Ryther JH (1962) Studies of marine planktonic diatoms: I. Cyclotella nana Hustedt, and *Detonula confervacea* (Cleve) gran. Can J Microbiol 8(2):229–239. https://doi.org/10.1139/m62-029

Harris EH (2001) Chlamydomonas as a model organism. Annu Rev Plant Biol 52:363–406. https://doi.org/10.1146/annurev.arplant.52.1.363

Hegemann P, Fuhrmann M, Kateriya S (2001) Minireview algal sensory photoreceptors 1. J Phycol 37

Jeffrey SW, Humphrey GF (1975) New spectrophotometric equations for determining chlorophylls a, b, C1 and C2 in higher plants, algae and natural phytoplankton. Biochem Physiol Pflanz 167(2):191–194. https://doi.org/10.1016/S0015-3796(17)30778-3

Levitan O, Dinamarca J, Zelzion E, Lun DS, Tiago Guerra L, Kim MK, Kim J, Van Mooy BAS, Bhattacharya D, Falkowski PG (2015) Remodeling of intermediate metabolism in the diatom phaeodactylum tricornutum under nitrogen stress. Proc Natl Acad Sci 112(2):412–417. https://doi.org/10.1073/pnas.1419818112

Liang YK, Dubos C, Dodd IC, Holroyd GH, Hetherington AM, Campbell MM (2005) AtMYB61, an R2R3-MYB transcription factor controlling stomatal aperture in *Arabidopsis thaliana*. Curr Biol. https://doi.org/10.1016/j.cub.2005.06.041

Lindemose S, O'Shea C, Jensen MK, Skriver K (2013) Structure, function and networks of transcription factors involved in abiotic stress responses. Int J Mol Sci. https://doi.org/10.3390/ijms14035842

Liu X, Li L, Li M, Liangchen Su, Lian S, Zhang B, Li X, Ge K, Li L (2018) AhGLK1 affects chlorophyll biosynthesis and photosynthesis in peanut leaves during recovery from drought. Sci Rep. https://doi.org/10.1038/s41598-018-20542-7

Long SP, Humphries S, Falkowski PG (1994) Photoinhibition of photosynthesis in nature. Annu Rev Plant Physiol Plant Mol Biol 45(1):633–662. https://doi.org/10.1146/ANNUREV.PP.45.060194.003221

Matthijs M, Fabris M, Obata T, Foubert I, Franco-Zorrilla JM, Solano R, Fernie AR, Vyverman W, Goossens A (2017) The transcription factor BZIP14 regulates the TCA cycle in the diatom *Phaeodactylum tricornutum*. EMBO J 36(11):1559–1576. https://doi.org/10.15252/embj.201696392

McLachlan J (1964) Some considerations of the growth of marine algae in artificial media. Can J Microbiol 10(5):769–782. https://doi.org/10.1139/m64-098

Meyerowitz EM (2001) Prehistory and history of Arabidopsis research. Plant Physiol 125(1):15–19. https://doi.org/10.1104/pp.125.1.15

Nguyen B, Tanious FA, David Wilson W (2007) Biosensor-surface plasmon resonance: quantitative analysis of small molecule-nucleic acid interactions. Methods 42(2):150–161. https://doi.org/10.1016/j.ymeth.2006.09.009

Nott A, Jung HS, Koussevitzky S, Chory J (2006) Plastid-to-nucleus retrograde signaling. Annu Rev Plant Biol. https://doi.org/10.1146/annurev.arplant.57.032905.105310

Pfannschmidt T (2003) Chloroplast redox signals: how photosynthesis controls its own genes. Trends Plant Sci. https://doi.org/10.1016/S1360-1385(02)00005-5

Pfannschmidt T, Bräutigam K, Wagner R, Dietzel L, Schröter Y, Steiner S, Nykytenko A (2009) Potential regulation of gene expression in photosynthetic cells by redox and energy state: approaches

towards better understanding. Ann Bot 103(4):599–607. https://doi.org/10.1093/aob/mcn081

Rayko E, Maumus F, Maheswari U, Jabbari K, Bowler C (2010) Transcription factor families inferred from genome sequences of photosynthetic stramenopiles. New Phytol 188(1):52–66. https://doi.org/10.1111/j.1469-8137.2010.03371.x

Rochaix JD (1995) *Chlamydomonas reinhardtii* as the photosynthetic yeast. Annu Rev Genet. https://doi.org/10.1146/annurev.ge.29.120195.001233

Soitamo AJ, Piippo M, Allahverdiyeva Y, Battchikova N, Aro EM (2008) Light has a specific role in modulating arabidopsis gene expression at low temperature. BMC Plant Biol. https://doi.org/10.1186/1471-2229-8-13

Sukenik A, Bennett J, Falkowski P (1987) Light-saturated photosynthesis—limitation by electron transport or carbon fixation? Biochim Biophys Acta Bioenerg 891(3):205–215. https://doi.org/10.1016/0005-2728(87)90216-7

Wang ZY, Tobin EM (1998) Constitutive expression of the CIRCADIAN CLOCK ASSOCIATED 1 (CCA1) gene disrupts circadian rhythms and suppresses its own expression. Cell. https://doi.org/10.1016/S0092-8674(00)81464-6

Zallen DT (1993) The 'Light' organism for the job: green algae and photosynthesis research. J Hist Biol 26(2):269–279. https://doi.org/10.1007/BF01061970

Zhou C, Li C (2016) A novel R2R3-MYB transcription factor BpMYB106 of birch (*Betula platyphylla*) confers increased photosynthesis and growth rate through up-regulating photosynthetic gene expression. Front Plant Sci 7(MAR2016):315. https://doi.org/10.3389/fpls.2016.00315

Zoratti L, Karppinen K, Escobar AL, Häggman H, Jaakola L (2014) Light-controlled flavonoid biosynthesis in fruits. Front Plant Sci. https://doi.org/10.3389/fpls.2014.00534